Available online at www.sciencedirect.com
ScienceDirect
Acta Materialia 56 (2008) 4869–4875
Acta MATERIALIA
www.elsevier.com/locate/actamat

Optical constants of new amorphous As–Ge–Se–Sb thin films

A. Dahshan [a,*], K.A. Aly [b]

[a] Department of Physics, Faculty of Science, Suez Canal University, Port Said, Egypt
[b] Physics Department, Faculty of Science, Al-Azhar University, Assiut Branch, Assiut, Egypt

Received 26 January 2008; received in revised form 23 May 2008; accepted 2 June 2008
Available online 7 July 2008

Abstract

The present paper reports the effect of replacement of selenium by antimony on the optical constants of new quaternary chalcogenide $As_{14}Ge_{14}Se_{72-x}Sb_x$ (where $x = 3$, 6, 9, 12 and 15 at.%) thin films. Films of $As_{14}Ge_{14}Se_{72-x}Sb_x$ glasses were prepared by thermal evaporation of the bulk samples. The transmission spectra, $T(\lambda)$, of the films at normal incidence were obtained in the spectral region from 400 to 2500 nm. A straightforward analysis proposed by Swanepoel, based on the use of the maxima and minima of the interference fringes, has been applied to derive the real and imaginary parts of the complex index of refraction and also the film thickness. Increasing antimony content is found to affect the refractive index and the extinction coefficient of the $As_{14}Ge_{14}Se_{72-x}Sb_x$ films. Optical absorption measurements show that the fundamental absorption edge is a function of composition. With increasing antimony content the refractive index increases while the optical band gap decreases.

Keywords: Amorphous; Thin films; Optical transmission

1. Introduction

Optical properties of thin films have been the subject of intense study during the last decades and great efforts have been made to develop the mathematical formulation describing the transmittance and reflectance of different optical systems [1,2]. Among the existing methods for determining the optical constants, those based exclusively on the optical transmission spectra at normal incidence have been applied to different crystalline and amorphous materials deposited on transparent substrates in the form of thin films [3–8]. These relatively simple methods do not require any previous knowledge of the thickness of the films, and are fairly accurate with the thickness and refractive index being determinable to within about 1% [5]. They do, however, assume that the film has a uniform thickness which, when absent, leads to less accurate results and even serious errors.

The thermal stability, crystallization kinetics, theoretical and experimental characterization of As–Ge–Se–Sb glasses in form of bulk and thin films have been described in our previous papers [9,10].

The present study is undertaken to investigate the influence of addition of antimony (3, 6, 9, 12 and 15 at.%), which is higher in atomic weight (more electropositive) than selenium on the complex refractive index ($n_c = n - ik$) and other optical constants of the amorphous $As_{14}Ge_{14}Se_{72-x}Sb_x$ thin films. It can readily be seen that the composition $As_{14}Ge_{14}Se_{63}Sb_9$ represents the so-called stoichiometric composition; with this composition as a reference, glasses with Se content of more than 63 at.% can be called Se-rich glasses and those with Se content of less than 63 at.% can be called As-rich glasses.

2. Experimental details

Different compositions of bulk $As_{14}Ge_{14}Se_{72-x}Sb_x$ (where $x = 3$, 6, 9, 12 and 15 at.%) chalcogenide glasses were prepared from their components of high-purity

* Corresponding author. Tel.: +20 181645141.
E-mail addresses: adahshan73@gmail.com (A. Dahshan), kamalaly2001@gmail.com (K.A. Aly).

1359-6454/$34.00 © 2008 Acta Materialia Inc. Published by Elsevier Ltd. All rights reserved.
doi:10.1016/j.actamat.2008.06.001

(99.999%) by the melt quenching technique. The elements were heated together in an evacuated (10^{-3} Pa) silica ampoule up to 1175 K, and then the ampoule temperature kept constant for about 24 h. During the course of heating, the ampoule was shaken several times to maintain the uniformity of the melt. Finally, the ampoule was quenched into ice cooled water to avoid crystallization.

Thin films of $As_{14}Ge_{14}Se_{72-x}Sb_x$ were prepared by thermal evaporation of the bulk samples. The thermal evaporation process was performed inside a coating (Edward 306E) system, at a pressure of approximately 10^{-3} Pa. During the deposition process (at normal incidence), the substrates were suitably rotated in order to obtain films of uniform thickness.

The elemental compositions of the investigated specimens were checked using the energy dispersive X-ray (Link Analytical Edx) spectroscopy. The deviations in the elemental compositions of the evaporated thin films from their initial bulk specimens were found not to exceed 1.0 at.%. The amorphous state of the films was checked using an X-ray (Philips type 1710 with Cu as a target and Ni as a filter, $\lambda = 1.5418$ Å) diffractometer. The absence of crystalline peaks confirms the amorphous state of the prepared samples.

A double-beam (Jasco V-630) spectrophotometer was used to measure the transmittance for the prepared films in the spectral range of wavelength from 400 to 2500 nm. Without a glass substrate in the reference beam, the measured transmittance spectra were used to calculate the optical constants of the films. In the present work, the envelope method suggested by Swanepoel [5] has been applied.

3. Results and discussion

3.1. Calculation of the refractive index and film thickness

The optical system under consideration corresponds to homogeneous and uniform thin films, deposited on thick transparent substrates. The thermally evaporated films have thickness d and complex refractive index $n_c = n - ik$, where n is the refractive index and k the extinction coefficient. The thickness of the substrate is several orders of magnitude larger than d, and its refractive index is symbolized by s. The substrate is considered to be perfectly smooth, but thick enough so that in practice the planes are not perfectly parallel so that all interference effects arising from the substrate are destroyed. The system is surrounded by air with refractive index $n_o = 1$. Taking all the multiple reflections at the three interfaces into account, it can be shown that in the case $k^2 \ll n^2$, the transmission T at normal incidence is given by [11–13]:

$$T = \frac{Ax}{B - Cx\cos(\phi) + Dx^2} \tag{1}$$

where $A = 16n^2s$, $B = (n+1)^3\ (n+s^2)$, $C = 2(n^2-1)(n^2-s^2)$, $D = (n-1)^3(n-s^2)$, $\phi = 4\pi nd/\lambda$ and $x = \exp(-\alpha d)$. The values of the transmission at the maxima and minima of the interference fringes can be obtained from Eq. (1) by setting the interference condition $\cos\phi = +1$ for maxima (T_M) and $\cos\phi = -1$ for minima (T_m).

Fig. 1 shows the measured transmittance (T) spectra, the created envelopes T_M and T_m, and the geometric mean, $T_\alpha = \sqrt{T_M T_m}$ in the spectral region with interference fringes for the $As_{14}Ge_{14}Se_{72-x}Sb_x$ (where $x = 3$, 9 and 15 at.%) thin films, according to Swanepoel's method based on the idea of Manifacier et al. [14]. The first approximate value of the refractive index of the film n_1 in the spectral region of medium and weak absorption can be calculated from the following expression:

$$n_1 = \sqrt{N + \sqrt{N^2 - s^2}} \tag{2}$$

where

$$N = 2s\frac{T_M - T_m}{T_M T_m} + \frac{s^2+1}{2}$$

here T_M and T_m are the transmission maximum and the corresponding minimum at a certain wavelength λ. Alternatively, one of these values is an experimental interference maximum (minimum) and the other one is derived from the corresponding envelope. Both envelopes being computer-generated using the OriginLab (version 7) program. The index of refraction of the substrate s at each wavelength is derived from T_s (λ), using the equation [15]:

$$s = \frac{1}{T_s} + \sqrt{\frac{1}{T_s^2} - 1} \tag{3}$$

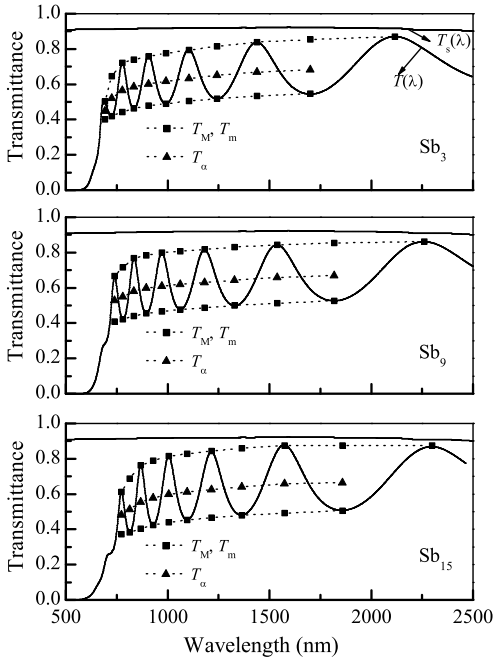

Fig. 1. Transmission spectra of $As_{14}Ge_{14}Se_{72-x}Sb_x$ ($x = 3$, 9 and 15 at.%) thin films. The average thicknesses of these samples are 810, 832 and 818 nm for $x = 3$, 9 and 15 at.%, respectively. Curves T_M, T_m and T_α, according to the text. T_s is the transmission of the substrate alone.

The calculated values of the refractive index (n_1), using Eq. (2) are listed in Table 1. The accuracy of this initial estimation of the refractive index is improved after calculating d, as will be explained below. Now, it is necessary to take into account the basic equation for the interference fringes:

$$2nd = m_o\lambda \tag{4}$$

where the order number m_o is an integer for maxima and a half-integer for minima. Moreover, if n_{c1} and n_{c2} are the refractive indices at two adjacent maxima (or minima) at λ_1 and λ_2, then the film thickness can be expressed as:

$$d = \frac{\lambda_1 \cdot \lambda_2}{2(n_{c2}\lambda_1 - n_{c1} \cdot \lambda_2)} \tag{5}$$

The values of d determined by this equation for different samples are listed as d_1 in Table 1. The last value deviates considerably from the other values and must consequently be rejected. The average value ($\overline{d_1}$) of d_1 (ignoring the last value), can now be used, along with n_1, to calculate m_o for the different maxima and minima using Eq. (4). The accuracy of the film thickness can now be significantly increased by taking the corresponding exact integer or half-integer values of m_o associated with each extreme point (see Fig. 1) and deriving a new thickness (d_2). The values of the thickness in this way have a smaller dispersion. It should be emphasized that the accuracy of the final thickness is better than 1% (see Table 1).

With the accurate values of m_o and the average value ($\overline{d_2}$) of d_2, Eq. (4) can then be solved for n at each λ and, thus, the final values of the refractive index n_2 are obtained. These values are listed in Table 1. Fig. 2 illustrates the dependence of the refractive index n on wavelength for different compositions of the amorphous $As_{14}Ge_{14}Se_{72-x}Sb_x$ (where $x = 3$, 9 and 15 at.%) thin films. The relative error in n, $\Delta n/n$, does not exceed the precision of the measurements $\Delta T/T$ (±1%). Now, the values of n_2 can be fitted to a function such as the two-term Cauchy dispersion relationship [16]:

$$n(\lambda) = a + \frac{b}{\lambda^2} \tag{6}$$

which can then be used to extrapolate the wavelength dependence beyond the range of measurement (see Fig. 2). The least-squares fit of n_2 for the different samples listed in

Table 1
Values of λ, T_s, T_M, T_m, n_1, d_1, m_o, d_2 and n_2 for $As_{14}Ge_{14}Se_{72-x}Sb_x$ ($x = 3$, 9 and 15 at.%) thin films from transmission spectra of Fig. 1

Sb content	λ	T_s	T_M	T_m	n_1	d_1	m_o	m	d_2	n_2
3 at.%	1700	0.918	0.854	0.546	2.646		2.55	2.5	803	2.623
	1440	0.918	0.838	0.533	2.673		3.04	3	808	2.667
	1243	0.918	0.816	0.519	2.695	818	3.55	3.5	807	2.685
	1104	0.918	0.794	0.506	2.713	831	4.02	4	814	2.726
	992	0.918	0.775	0.490	2.752	824	4.54	4.5	811	2.756
	907	0.916	0.759	0.478	2.789	810	5.03	5	813	2.799
	834	0.914	0.739	0.464	2.829	810	5.54	5.5	811	2.831
	778	0.914	0.722	0.442	2.913	747	6.13	6	801	2.881
	726	0.912	0.646	0.420	2.873	885	6.47	6.5	821	2.913
	693	0.912	0.502	0.400	2.479	–	–	–	–	–
	$\bar{d}1 = 818, \delta1 = 40$ *nm* (4.9%); $\bar{d}2 = 810,\ \delta2 = 6$ *nm* (0.7%)									
9 at.%	1818	0.918	0.853	0.526	2.727		2.50	2.5	833	2.712
	1538	0.918	0.844	0.513	2.768		3.00	3	833	2.753
	1329	0.918	0.830	0.499	2.808	816	3.52	3.5	828	2.775
	1181	0.918	0.819	0.488	2.835	832	4.00	4	833	2.819
	1063	0.918	0.808	0.476	2.879	840	4.52	4.5	831	2.854
	972	0.916	0.800	0.466	2.924	824	5.02	5	831	2.899
	896	0.914	0.784	0.456	2.956	846	5.50	5.5	834	2.940
	835	0.914	0.768	0.439	3.018	824	6.03	6	830	2.989
	781	0.912	0.717	0.421	3.032	857	6.48	6.5	837	3.029
	740	0.912	0.666	0.410	2.924	–	–	–	–	–
	$\bar{d}1 = 834, \delta1 = 14$ *nm* (1.7%); $\bar{d}2 = 832,\ \delta2 = 2.6$ *nm* (0.3%)									
15 at.%	1858	0.922	0.874	0.506	2.826		2.50	2.5	822	2.839
	1574	0.921	0.874	0.493	2.893		3.03	3	816	2.886
	1364	0.92	0.859	0.479	2.935	793	3.54	3.5	813	2.918
	1215	0.919	0.845	0.466	2.973	821	4.03	4	817	2.971
	1097	0.919	0.828	0.452	3.024	826	4.54	4.5	816	3.017
	1005	0.918	0.815	0.439	3.077	814	5.04	5	817	3.071
	928	0.917	0.789	0.425	3.116	832	5.53	5.5	819	3.120
	868	0.916	0.762	0.404	3.198	803	6.06	6	814	3.183
	813	0.915	0.687	0.383	3.195	874	6.47	6.5	827	3.230
	773	0.914	0.612	0.372	3.055	–	–	–	–	–
	$\bar{d}1 = 823, \delta1 = 26$ *nm* (3.2%); $\bar{d}2 = 818,\ \delta2 = 4.3$ *nm* (0.5%)									

The underlined values of transmittance are those given in the transmittance spectra of Fig. 1 and the others are calculated by the envelope method.

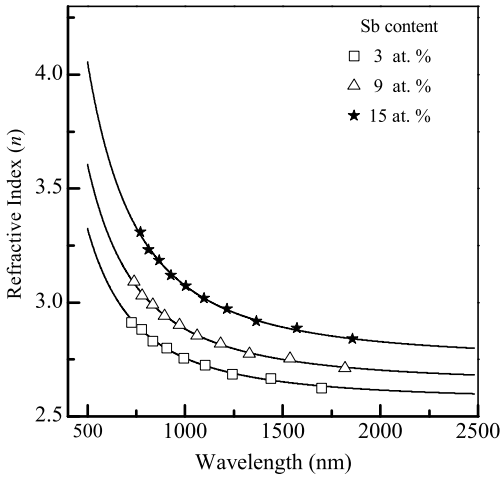

Fig. 2. Refractive index dispersion spectra for $As_{14}Ge_{14}Se_{72-x}Sb_x$ ($x = 3$, 9 and 15 at.%) thin films. Solid curves are determined according to Cauchy dispersion relationship [16].

Table 1, yields $n = 2.57 + (1.85 \times 10^5/\lambda^2)$ for $As_{14}Ge_{14}Se_{69}Sb_3$, $n = 2.64 + (2.4 \times 10^5/\lambda^2)$ for $As_{14}Ge_{14}Se_{63}Sb_9$, and $n = 2.75 + (3.28 \times 10^5/\lambda^2)$ for $As_{14}Ge_{14}Se_{57}Sb_{15}$ thin films.

The final values of the refractive index can be fitted to an appropriate function such as the Wemple–DiDomenico (WDD) dispersion relationship [17], i.e., to the single-oscillator model:

$$n^2(h\nu) = 1 + \frac{E_o E_d}{E_o^2 - (h\nu)^2} \tag{7}$$

where E_o is the single-oscillator energy and E_d is the dispersion energy or single-oscillator strength. By plotting $(n^2-1)^{-1}$ against $(h\nu)^2$ and fitting straight lines as shown in Fig. 3, E_o and E_d can be determined from the intercept, E_o/E_d, and the slope, $(E_o E_d)^{-1}$. The oscillator energy (E_o) is an average energy gap, and to a good approximation, scales with the optical band gap (E_g), $E_o \approx 2E_g$, as was found by Tanaka [18]. Fig. 3 also shows the values of the refractive index $n(0)$ at $h\nu = 0$ for the $As_{14}Ge_{14}Se_{72-x}Sb_x$ (where $x = 3$, 6, 9, 12 and 15 at.%) films. The obtained values of E_o, E_d and $n(0)$ are listed in Table 2. It was observed that the single-oscillator energy E_o and the dispersion energy E_d decrease with the increase in Sb content while refractive index $n(0)$ increases. An important achievement of the WDD model is that it relates the dispersion energy, E_d, to other physical parameters of the material through the following empirical relationship [17]:

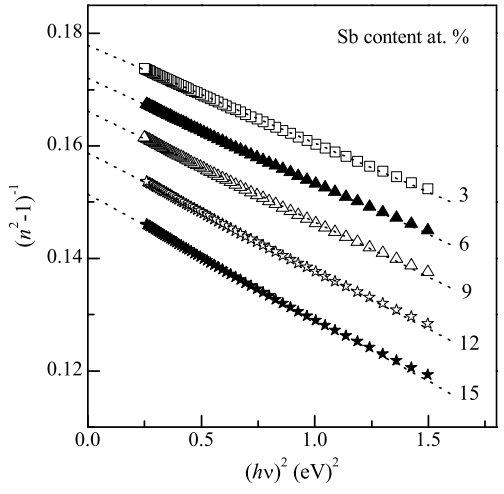

Fig. 3. Plots of refractive index factor $(n^2 - 1)^{-1}$ versus $(h\nu)^2$ for $As_{14}Ge_{14}Se_{72-x}Sb_x$ ($x = 3$, 6, 9, 12 and 15 at.%) thin films.

$$E_d = \beta N_c Z_a N_e (\text{eV}) \tag{8}$$

where N_c is the effective coordination number of the cation nearest-neighbour to the anion, Z_a is the formal chemical valency of the anion, N_e is the effective number of valence electrons per anion and $\beta = 0.37 \pm 0.04$ eV for covalent crystalline and amorphous materials. Therefore, in order to account for the compositional trended of E_d it is suggested that, the observed decrease in E_d with increasing Sb content is primarily due to the change in the ionicities, which increases with Sb content.

The dependence of the refractive index (n) on the lattice dielectric constant ε_L is given by [19]:

$$n^2 = \varepsilon_L - (e^2/\pi c^2)(N/m^*)\lambda^2 \tag{9}$$

where N/m^* is the ratio of the carrier concentration N to the effective mass m^*, c is the speed of light, and e is the electronic charge. The plots of n^2 versus λ^2 for the $As_{14}Ge_{14}Se_{72-x}Sb_x$ (where $x = 3$, 6, 9, 12 and 15 at.%) thin films as shown in Fig. 4 are linear, verifying Eq. (9). The values of ε_L and N/m^* were deduced from the extrapolation of these plots to $\lambda^2 = 0$ and from the slope of the graph, respectively. The obtained values for ε_L and N/m^* for the $As_{14}Ge_{14}Se_{72-x}Sb_x$ (where $x = 3$, 6, 9, 12 and 15 at.%) thin films are listed in Table 2.

Furthermore, a simple complementary graphical method for deriving the first-order number m_1 and film thickness d, based on Eq. (4) was also used. For this purpose Eq. (4) can now be written for the extremes of the spectrum as:

$$\frac{l}{2} = 2d \cdot \left(\frac{n}{\lambda}\right) - m_1 \tag{10}$$

where $l = 0$, 1, 2, 3, ... for the successive tangent points, starting from the long wavelength end and m_1 is the order number of the first ($l = 0$) tangent point considered, where m_1 is an integer or a half-integer for the upper or lower tan-

Table 2
Wemple–DiDomenico dispersion parameters (E_o and E_d), values of the refractive index $n(0)$ extrapolated at $h\nu = 0$, lattice dielectric constant (ε_L) and the N/m^* ratio for $As_{14}Ge_{14}Se_{72-x}Sb_x$ ($x = 3$, 6, 9, 12 and 15 at.%) thin films

Composition	E_o (eV)	E_d (eV)	$n(0)$	ε_L	N/m^* (10^{31}/cm^3)
$As_{14}Ge_{14}Se_{69}Sb_3$	3.20	17.97	2.57	6.99	4.70
$As_{14}Ge_{14}Se_{66}Sb_6$	3.06	17.75	2.61	7.23	5.19
$As_{14}Ge_{14}Se_{63}Sb_9$	2.91	17.52	2.65	7.50	6.15
$As_{14}Ge_{14}Se_{60}Sb_{12}$	2.76	17.38	2.71	7.87	7.27
$As_{14}Ge_{14}Se_{57}Sb_{15}$	2.61	17.24	2.76	8.25	8.44

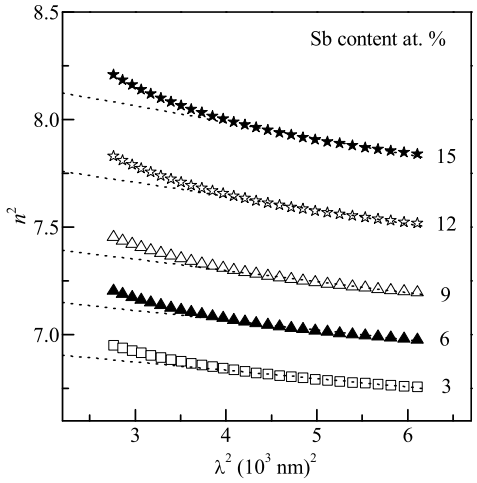

Fig. 4. Plots of n^2 versus λ^2 for $As_{14}Ge_{14}Se_{72-x}Sb_x$ ($x = 3$, 6, 9, 12 and 15 at.%) thin films.

gent points, respectively. Therefore, by plotting ($l/2$) versus (n/λ) we obtain a straight line with slope $2d$ and cut-off on the vertical axis at $-m_1$ as shown in Fig. 5. The obtained values of $2d$ and m_1 for the $As_{14}Ge_{14}Se_{72-x}Sb_x$ (where $x = 3$, 9 and 15 at.%) thin films are displayed as shown in this figure.

3.2. Determination of the extinction coefficient and optical band gap

Continuing with the description of the data processing method, when there is no substrate in the reference beam and the values of the refractive index (n) and the thickness (d) of the films are already known, the absorption coefficient α is derived using the interference-free transmission spectrum T_α (see Fig. 1) over the whole spectral range, using the well-known equation suggested by Connell and Lewis [20]:

$$\alpha = -\frac{1}{d}\ln\left(\frac{1}{B}\{A + [A^2 + 2BT_\alpha(1 - R_2R_3)]^{1/2}\}\right) \quad (11)$$

where $A = (R_1 - 1)(R_2 - 1)(R_3 - 1)$, $B = 2T_\alpha(R_1\ R_2 + R_1\ R_3 - 2R_1\ R_2R_3)$, R_1 is the reflectance of the air–film interface ($R_1 = [(1 - n)/(1 + n)]^2$), R_2 is the reflectance of film–substrate interface ($R_2 = [(n - s)/\ (n + s)]^2$) and R_3 is the reflectance of the substrate–air interface ($R_3 = [(s - 1)/(s + 1)]^2$). To complete the calculations of the optical constants, the extinction coefficient k is calculated using the values of α and λ by the relation:

$$k = \alpha\lambda/4\pi \quad (12)$$

Fig. 6 illustrates the dependence of k on the wavelength for $As_{14}Ge_{14}Se_{72-x}Sb_x$ ($x = 3$, 9 and 15 at.%) thin films. For $\alpha \leqslant 10^5\ cm^{-1}$, the imaginary part of the complex index of refraction is much less than n, so that the previous expressions used to calculate the reflectance are valid. In the region of strong absorption, the interference fringes disappear; in other words, for very large α the three curves T_M, T_α and T_m converge to a single curve.

According to Tauc's relation [21,22] for allowed non-direct transitions, the photon energy dependence of the absorption coefficient can be described by:

$$(\alpha h\nu)^{1/2} = B(h\nu - E_g) \quad (13)$$

where B is a parameter that depends on the transition probability and E_g is the optical energy gap. Fig. 7 shows the absorption coefficient in the form of $(\alpha h\nu)^{1/2}$ versus $h\nu$ for the $As_{14}Ge_{14}Se_{72-x}Sb_x$ ($x = 3$, 9 and 15 at.%) films. The intercepts of the straight lines with the photon energy axis yield the values of the optical band gap. The variation

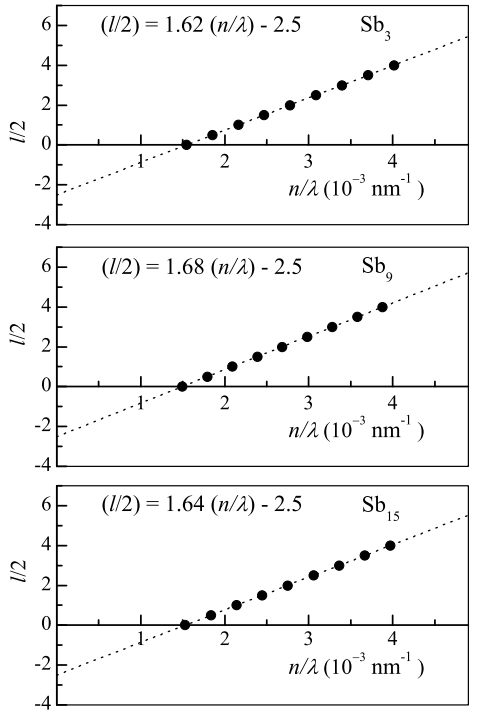

Fig. 5. Plots of ($l/2$) versus (n/λ) to determine the film thickness and the first-order number m_1 for $As_{14}Ge_{14}Se_{72-x}Sb_x$ ($x = 3$, 9 and 15 at.%) thin films.

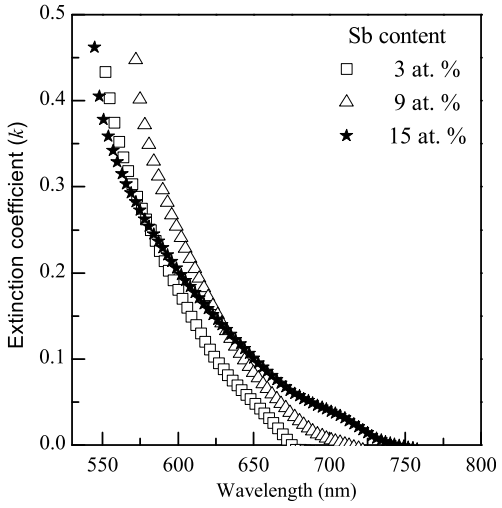

Fig. 6. Extinction coefficient k versus λ for $As_{14}Ge_{14}Se_{72-x}Sb_x$ ($x = 3$, 9 and 15 at.%) thin films.

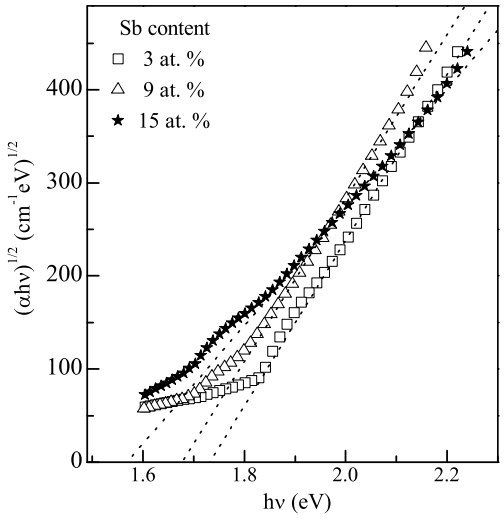

Fig. 7. Dependence of $(\alpha h\nu)^{1/2}$ on photon energy ($h\nu$) for $As_{14}Ge_{14}Se_{72-x}Sb_x$ ($x = 3$, 9 and 15 at.%) thin films from which the optical band gap (E_g) is estimated (Tauc extrapolation).

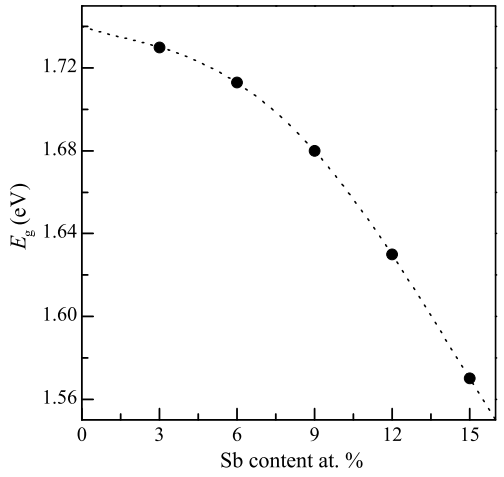

Fig. 8. Variation in the optical band gap (E_g) as a function of Sb content for $As_{14}Ge_{14}Se_{72-x}Sb_x$ ($x = 3$, 6, 9, 12 and 15 at.%) thin films.

of E_g as a function of Sb content for the $As_{14}Ge_{14}Se_{72-x}Sb_x$ (where $x = 3$, 6, 9, 12 and 15 at.%) thin films is depicted in Fig. 8. From this figure, it is clear that E_g decreases with increasing Sb content for the investigated films. The decrease in the optical band gap with increasing Sb content can be interpreted on the basis of the chemical-bond approach proposed by Bicerano and Ovshinsky [23].

The bond energies of the various bonds involved, namely, Ge–Se, Sb–Se, As–Se and Se–Se are, respectively, equal to 49.44, 43.97, 41.69 and 44.04 kcal/mol. [10]. For Se-rich glasses (i.e., glasses with Sb content less than 9 at.%), Ge, Sb and As atoms bond to Se atoms to form $GeSe_2$, Sb_2Se_3 and As_2Se_3 structural units, respectively. After forming these bonds there were still unsatisfied Se valences which must be satisfied by the formation of Se–Se bonds (Se chains). The composition $As_{14}Ge_{14}Se_{63}Sb_9$ can be envisaged to be made up of completely cross-linked three-dimensional structural units of $GeSe_2$, Sb_2Se_3 and As_2Se_3 only, with neither Se nor As in excess [10]. With the increasing Sb content in the As-rich glasses (i.e., glasses with Sb content more than 9 at.%), the Sb_2Se_3/As_2Se_3 ratio progressively increases and some of the original As_2Se_3 structural units are replaced by As.

The optical gap could be obtained from addition of the partial optical gaps of the different structural phases formed inside the film. With increasing Sb content from 3 up to 9 at.%, Sb_2Se_3 ($E_g = 1.28$ eV [24]) phase replaces the Se ($E_g = 1.95$ eV) phase which is behind the reduction of the optical gap. Increasing Sb content more than 9 at.%, both As–As ($E_g = 1.15$ eV) and Sb_2Se_3 phases replace the As_2Se_3 ($E_g = 1.68$ eV [25]) phase, which in turns decreases the optical gap of the films with increasing Sb content.

4. Conclusions

Optical data indicated that the allowed non-direct gap is responsible for the photons absorption in the $As_{14}Ge_{14}Se_{72-x}Sb_x$ thin films. The optical band gap has been determined from the spectral dependence of the absorption coefficient using the Tauc formula. It was found that the optical band gap (E_g), the single-oscillator energy (E_o) and the dispersion energy (E_d) decrease, while the refractive index increases on increasing the Sb content in the films. The dispersion of the refractive index is discussed in terms of the single-oscillator Wemple and DiDomenico model. The chemical-bond approach can be applied successfully to interpret the decrease of the optical gap with increasing Sb content.

References

[1] Swanepoel RJ. Phys E: Sci Instrum 1984;17:896.
[2] Gonzalez-Leal JM, Prieto-Alcon R, Stuchlik M, Vlcek M, Elliott SR, Marquez E. Opt Mater 2004;27:147.
[3] Aly KA, Dahshan A, Abousehly AM. Philos Mag 2008;88:1. 47.
[4] Manifacier JC, Gasiot J, Fillard JP. J Phys E: Sci Instrum 1976;9:1002.
[5] Swanepoel RJ. Phys E: Sci Instrum 1983;16:1214.
[6] Hamman M, Harith MA, Osman WH. Solid State Commun 1986;59:271.
[7] Kalomiros JA. Spyridelis J Phys Status Solidi a 1988;107:633.
[8] Marquez E, Ramirez-Malo J, Villares P, Jimenez-Garay R, Ewen PJS, Owen AEJ. Phys D: Appl Phys 1992;25:535.
[9] Dahshan A. J Non-cryst Solids 2008;354:3034.
[10] Dahshan A, Aly KA. Philos Mag 2008;88:3. 361.
[11] Marquez E, Bernal-Oliva AM, Gonzalez-Leal JM, Prieto-Alcon R, Jimenez-Garay RJ. Non-cryst Solids 1997;222:250.
[12] Marquez E, Ramirez-Malo J, Villares P, Jimenez-Garay R, Ewen PJS, Owen AE. J Phys D: Appl Phys 1992;25:535.
[13] Heavens S. Optical properties of thin solid films. London: Butterworths; 1955.
[14] Manifacier JC, Gasiot J, Fillard JP. J Phys E: Sci Instrum 1976;9:1002.
[15] Jenkins FA, White HE. Fundamentals of optics. New York: McGraw-Hill; 1957.
[16] Moss TS. Optical properties of semiconductors. London: Butterworths; 1959.

[17] Wemple SH, DiDomenico M. Phys Rev 1971;B3:1338.
[18] Tanaka K. Thin Solid Films 1980;66:271.
[19] Kumar G, Thomas J, George N, Kumar B, Shnan P, Npoori V, et al. Phys Chem Glasses 2001;41:89.
[20] Connell GAN, Lewis AJ. Phys Status Solidi b 1973;60:291.
[21] Davis EA, Mott NF. Philos Mag 1970;22:903.
[22] Fritzsche H. Philos Mag B 1993;68:561.
[23] Bicerano J, Ovshinsky SR. J Non-cryst Solids 1985;74:75.
[24] Zayed HA, Abo-Elsoud AM, Ibrahim AM, Kenawy MA. Thin Solid Films 1994;247:94.
[25] Moharram AH, Othman AA, Amer HH, Dahshan AJ. Non-cryst Solids 2006;352:2187.